

Mapping Simocyclinone D8 Interaction with DNA Gyrase: Evidence for a New Binding Site on GyrB^{∇†}

C. Sissi,^{1*} E. Vazquez,¹ A. Chemello,¹ L. A. Mitchenall,² A. Maxwell,² and M. Palumbo¹

Department of Pharmaceutical Sciences, University of Padova, Via Marzolo, Padua 5-35131, Italy,¹ and Department of Biological Chemistry, John Innes Centre, Colney, Norwich NR4 7UH, United Kingdom²

Received 13 July 2009/Returned for modification 8 September 2009/Accepted 16 October 2009

Simocyclinone D8, a coumarin derivative isolated from *Streptomyces antibioticus* Tü 6040, represents an interesting new antiproliferative agent. It was originally suggested that this drug recognizes the GyrA subunit and interferes with the gyrase catalytic cycle by preventing its binding to DNA. To further characterize the mode of action of this antibiotic, we investigated its binding to the reconstituted DNA gyrase (A₂B₂) as well as to its GyrA and GyrB subunits and the individual domains of these proteins, by performing protein melting and proteolytic digestion studies as well as inhibition assays. Two binding sites were identified, one (anticipated) in the N-terminal domain of GyrA (GyrA59) and the other (unexpected) at the C-terminal domain of GyrB (GyrB47). Stabilization of the A subunit appears to be considerably more effective than stabilization of the B subunit. Our data suggest that these two distinct sites could cooperate in the reconstituted enzyme.

Resistance to antibiotics is a constantly increasing clinical concern, particularly in hospitals and other health care settings (16, 22). In fact, antibiotic-resistant pathogens cause serious infections for which there are limited therapeutic interventions and that are often life threatening. Hence, the discovery and development of new, effective antibacterial drugs that possibly exhibit new mechanisms of action represent challenging and urgent goals. Possible successful approaches include (i) the exploitation of new drug targets in the pathogen and (ii) the identification of drugs that act at a novel site(s) of known targets (35). In either case, detailed information on the molecular mechanism(s) of drug action is required to rationally develop new effective agents.

In this connection, a major target for antimicrobial intervention is DNA gyrase (19). This enzyme is a prokaryotic type II topoisomerase that modulates the topological state of DNA through cleaving and resealing steps (24, 31). Besides performing reactions such as decatenation, unknotting, and relaxation common to the type II family members, DNA gyrase is also able to introduce negative supercoils, a reaction coupled to ATP hydrolysis (9, 10). DNA gyrase works as a tetramer (A₂B₂) formed by two A subunits (GyrA) and two B subunits (GyrB) (28). The catalytic tyrosine covalently linked to DNA in the cleavage complex is located in the N-terminal domain of GyrA (GyrA59). The C-terminal domain of GyrA (GyrA33) facilitates the wrapping of DNA around the enzyme. GyrB contains the ATP-binding and hydrolysis site in its N-terminal domain (GyrB43), whereas its C-terminal portion (GyrB47) is involved in DNA and GyrA binding.

A number of drugs are effective in impairing the activity of DNA gyrase (Fig. 1), among which the fluoroquinolones are

the therapeutically most relevant (3, 5). As suggested by biological and chemico-physical studies, they act at the cleavage site by trapping the cleavage complex and interacting principally with GyrA but also with GyrB and DNA (12, 27, 34, 37). Recently, the structures of a bacterial topoisomerase II with DNA and quinolones have been determined, confirming such a model (15).

Another well-known class of gyrase inhibitors is represented by the coumarin derivatives (20, 25, 36). Unfortunately, these compounds exhibit an inadequate pharmacological profile that prevents their widespread clinical application. This notwithstanding, they have proved very useful in providing detailed information on the mechanism of enzyme action and the molecular details of the drug-protein interaction (1, 11, 21). Compared to the quinolones, the coumarins act in a completely different way and at a distinct site located on GyrB, which partially overlaps the ATP-binding site (17). Thus, they prevent the ATP hydrolysis required for the enzymatic cycle.

More recently, novel angucyclinone-type DNA gyrase inhibitors, simocyclinone D4 and simocyclinone D8 (SD8), were isolated from the mycelium extract of *Streptomyces antibioticus* Tü 6040 (8, 13, 30, 38). They were shown to exhibit antiproliferative activity on gram-positive bacteria as well as on cancer cell lines (26, 29). In particular, SD8 has been shown to be even more effective than novobiocin at inhibiting gyrase-catalyzed supercoiling (7). Its mechanism of action is thought to involve the prevention of DNA binding by gyrase, and the structure of the N-terminal domain of GyrA (GyrA59) with SD8 bound has recently been solved (6). This novel mode of action suggests that SD8 is a potential new lead molecule for drug design.

In previous work, we utilized protein melting studies to characterize metal ion structural effects on both DNA gyrase subunits as well as quinolone binding to GyrA (32–34). In the study described here, we used the same experimental approach, along with activity assays and limited proteolysis experiments, as an effective means of monitoring the interaction of SD8 with DNA gyrase with the principal aim of locating the drug binding site(s) on the protein. As reference compounds,

* Corresponding author. Mailing address: Department of Pharmaceutical Sciences, University of Padova, Via Marzolo 5, Padova 35131, Italy. Phone: 390498275711. Fax: 390498275711. E-mail: claudia.sissi@unipd.it.

† Supplemental material for this article may be found at <http://aac.asm.org/>.

∇ Published ahead of print on 26 October 2009.

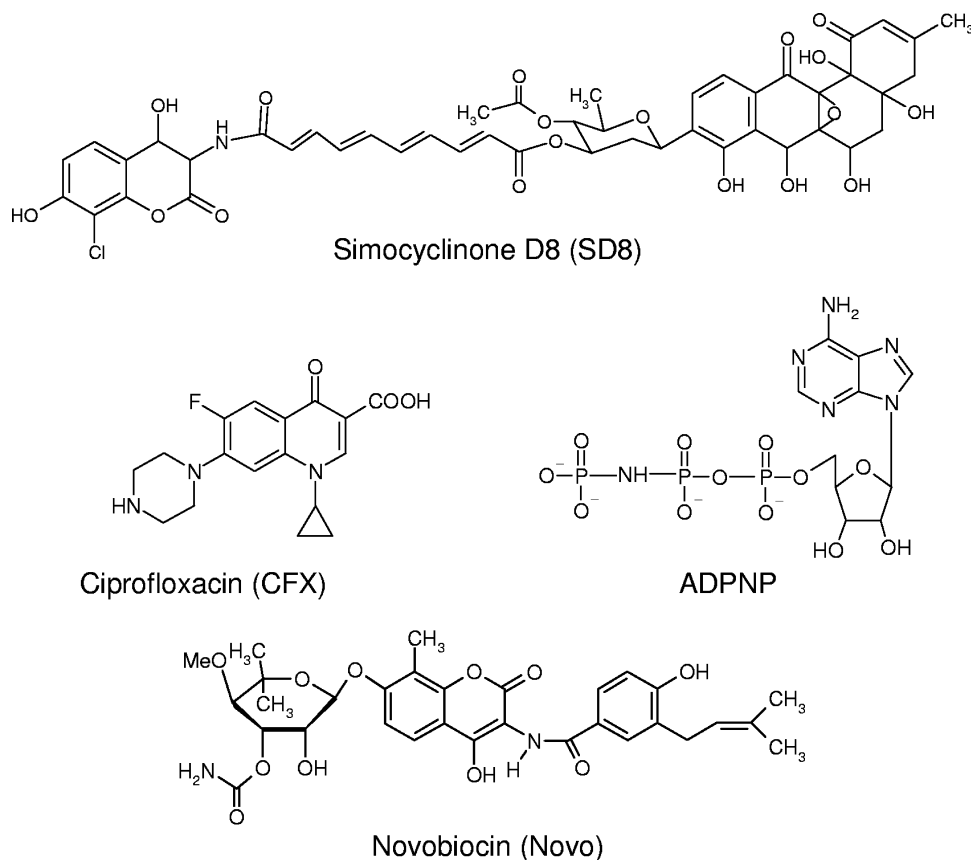


FIG. 1. Chemical structures of the DNA gyrase ligands tested.

we used the established gyrase inhibitors ciprofloxacin (CFX), a fluoroquinolone, and novobiocin (Novo), an aminocoumarin. Additionally, we also utilized ADPNP, a nonhydrolyzable analog of ATP, which efficiently binds to the enzyme (Fig. 1). Our results indicate that there are at least two sites for SD8 binding to DNA gyrase: one is located in the A subunit and the other is located in the B subunit.

MATERIALS AND METHODS

Proteins. All proteins were produced and purified according to previously reported protocols (23, 34). Protein concentrations were assessed from the UV absorbance and by the Bradford method (Bio-Rad).

Drugs. Ciprofloxacin was provided by Glaxo Wellcome (Verona, Italy). Stock solutions were made in double-distilled water and diluted to the working concentration in the desired buffer. SD8 was kindly provided by L. Heide, University of Tübingen. Stock solutions (≈ 1.5 mg/ml) were prepared in methanol. The solutions were further diluted with water, and their final concentrations were determined by measurement of the UV absorbance (ϵ at 345 nm = $11,000 \text{ M}^{-1} \text{ cm}^{-1}$). ADPNP was purchased from Sigma Chemical Co. (St. Louis, MO).

CD measurements. Circular dichroism (CD) measurements were performed in 10 mM Tris-HCl (pH 7.4)–20 mM KCl in the presence or the absence of MgCl_2 ions up to 4 mM. CD spectra were recorded by using 1- to 10-m μ m-path-length cells on a Jasco J810 spectropolarimeter. For each measurement, three scans were run and recorded with a 1-nm step resolution. The observed ellipticity was converted to the mean residue ellipticity, $[\theta]$, in degrees $\times \text{cm}^2 \times \text{dmol}^{-1}$. For the thermal denaturation experiments, protein solutions (≈ 0.01 mg/ml) were equilibrated at 25°C, and then the signal at 220 nm was recorded while the temperature was increased at 0.8°C/min and the protein solution was stirred to allow equilibration. The melting temperature (T_m) was determined by locating the maxima/minima of the first derivative of the curve describing the melting profile (CD versus temperature). The melting temper-

ature experiments were performed in triplicate, and the corresponding curves were practically superimposable.

Proteolysis measurements. Test proteins (3 μg) were mixed with 0.04 mg of trypsin in 50 mM Tris-HCl (pH 7.5)–50 mM KCl–4 mM MgCl_2 –4 mM dithiothreitol (DTT)–6.5% glycerol. After various times at 37°C, the reaction was stopped with 1 volume of stop mixture (62 mM Tris-HCl, pH 6.8, 2% sodium dodecyl sulfate [SDS], 10% glycerol, 0.1% bromophenol blue). Alternatively, proteolysis was performed by incubating the test proteins (1 to 3 μg) with thermolysin (0.16 mg/ml) for 30 s in 20 mM Tris-HCl–50 mM NaCl–10 mM CaCl_2 in a total volume of 10 μl . At the end of the incubation, samples were heated at 95°C and loaded onto a 12% SDS-polyacrylamide gel. The gels were stained with Coomassie brilliant blue, photographed, and quantified by use of a Bio-Rad Gel Doc 1000 apparatus.

DNA gyrase assays. Supercoiled plasmid pBR322 (0.125 μg ; Fermentas) was incubated with DNA gyrase (60 nM) in a total volume of 20 μl in 35 mM Tris-HCl (pH 7.5)–24 mM KCl–1.8 mM spermidine–2 mM DTT–0.1 mg/ml bovine serum albumin–6.5% (wt/vol) glycerol for 30 min at 37°C in the presence and the absence of increasing drug concentrations. The reaction products were resolved on 1% agarose gels in 0.5 \times TBE (45 mM Tris, 45 mM boric acid, 1 mM disodium EDTA), and the bands were visualized by ethidium bromide staining and photographed. The relative amounts of the different DNA topoisomers were quantified on the Bio-Rad Gel Doc 1000 apparatus.

Gel shift assay. A 5'-end-labeled DNA fragment corresponding to the sequence of pBR322 from positions 906 to 1064 was prepared by PCR. Before amplification, one synthetic primer was labeled with $[\gamma\text{-}^{32}\text{P}]\text{ATP}$ and T4 polynucleotide kinase in the appropriate buffer. The labeled DNA (2,000 cpm) was incubated with different amounts of protein at 25°C in the presence or the absence of SD8 in 50 mM Tris-HCl (pH 7.5)–4 mM MgCl_2 –55 mM KCl–5 mM DTT containing 5% glycerol. The mixture was incubated for 15 min at 25°C, loaded onto a 5% native polyacrylamide gel (75:1), and run at low voltage (35 V/cm) at 20°C in 90 mM Tris–90 mM boric acid–10 mM MgCl_2 . The bands were visualized by autoradiography and quantified with a Storm 840 apparatus (GE Healthcare).

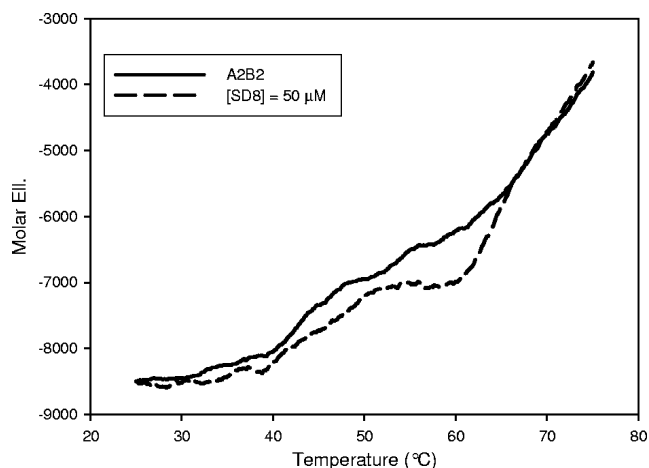


FIG. 2. Melting profiles of DNA gyrase acquired by reading the protein CD signal at 220 nm in 10 mM Tris-HCl (pH 7.5)–20 mM KCl–4 mM MgCl₂ in the absence (solid line) and in the presence (dashed line) of 50 μM SD8. The protein concentration was 0.05 μM. Mol. Ell., molar ellipticity.

RESULTS

SD8 efficiently binds to reconstituted DNA gyrase. The available data indicate that DNA gyrase is the biological target of SD8 (6, 7, 26). To monitor this interaction, we performed CD measurements using the reconstituted protein. Addition of SD8 did not induce significant changes in the CD spectra in the 200- to 250-nm range. Moreover, no apparent role was played by the presence of Mg²⁺ up to 4 mM. This points to the absence of extensive protein structural changes as a result of protein complexation. In our previous work, we were able to show gyrase-ligand interactions by monitoring the changes in protein thermal stability. Indeed, when SD8 was added to the reconstituted enzyme, we observed a dramatic shift to higher temperatures in the protein melting transitions (Fig. 2). This shift was a function of the SD8 concentration, thus suggesting

the formation of a protein-drug complex. The identification of the protein subdomains involved in the interaction with SD8 could be attempted from the analysis of the melting profiles. However, as we previously pointed out (32), it is not safe to perform such an analysis due to several overlapping transitions. Thus, we preferred to localize drug binding from the changes in the protein structure or thermal stability using each isolated protein subunit/domain.

SD8 affects the thermal transitions of both GyrA and GyrB.

The chiroptical properties of GyrA, GyrA59, GyrB, GyrB43, and GyrB47 have recently been investigated (33–34). Additionally, well-characterized ligands are available for GyrA (quinolones) and GyrB (Novo, ADPNP), and we utilized those ligands in our experiments to fully validate our results. In agreement with the behavior of the reconstituted enzyme discussed above, no significant changes in the protein CD spectra occurs upon addition of SD8 or the other ligands tested (data not shown). Again, here we detected drug binding from the changes in protein thermal stability upon addition of putative binders.

(i) **GyrA.** We previously reported that when the GyrA thermal melting profile was recorded in the presence or absence of CFX, a drug-mediated shift to a higher T_m was observed (34). However, neither of the other ligands tested was able to induce an appreciable modification in the thermal stability of GyrA. By using GyrA59 as a substrate, the same was true for ADPNP and Novo (see Fig. S1 in the supplemental material), whereas addition of SD8 produces a concentration-dependent increment in the protein T_m (Fig. 3A). This effect is not very remarkable (maximal change in T_m [ΔT_m] \approx 5.5°C), but the maximal variation occurred at a low drug concentration (10 μM). Additionally, by plotting T_m versus the SD8 concentrations, a sigmoidal curve was obtained, which suggests that a cooperative conformational change was produced upon drug binding (Fig. 3B).

(ii) **GyrB.** A clear modulation of the GyrB melting profile was observed in the presence of all ligands tested except CFX.

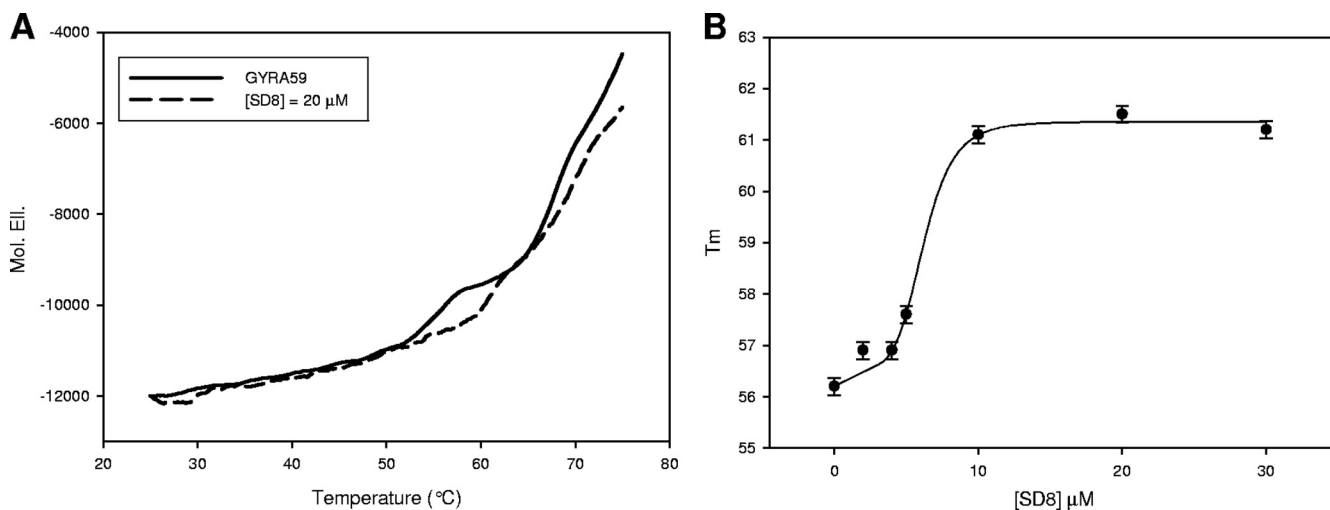


FIG. 3. SD8 modulation of the thermal stability of GyrA59 in 10 mM Tris-HCl (pH 7.5)–20 mM KCl–4 mM MgCl₂. (A) Melting profiles of GyrA59 acquired by reading the protein CD signal at 220 nm in the absence (solid line) and in the presence (dashed line) of SD8. The protein concentration was 0.2 μM. (B) Variation of the T_m for the thermal transition of GyrA59 as a function of SD8 concentration.

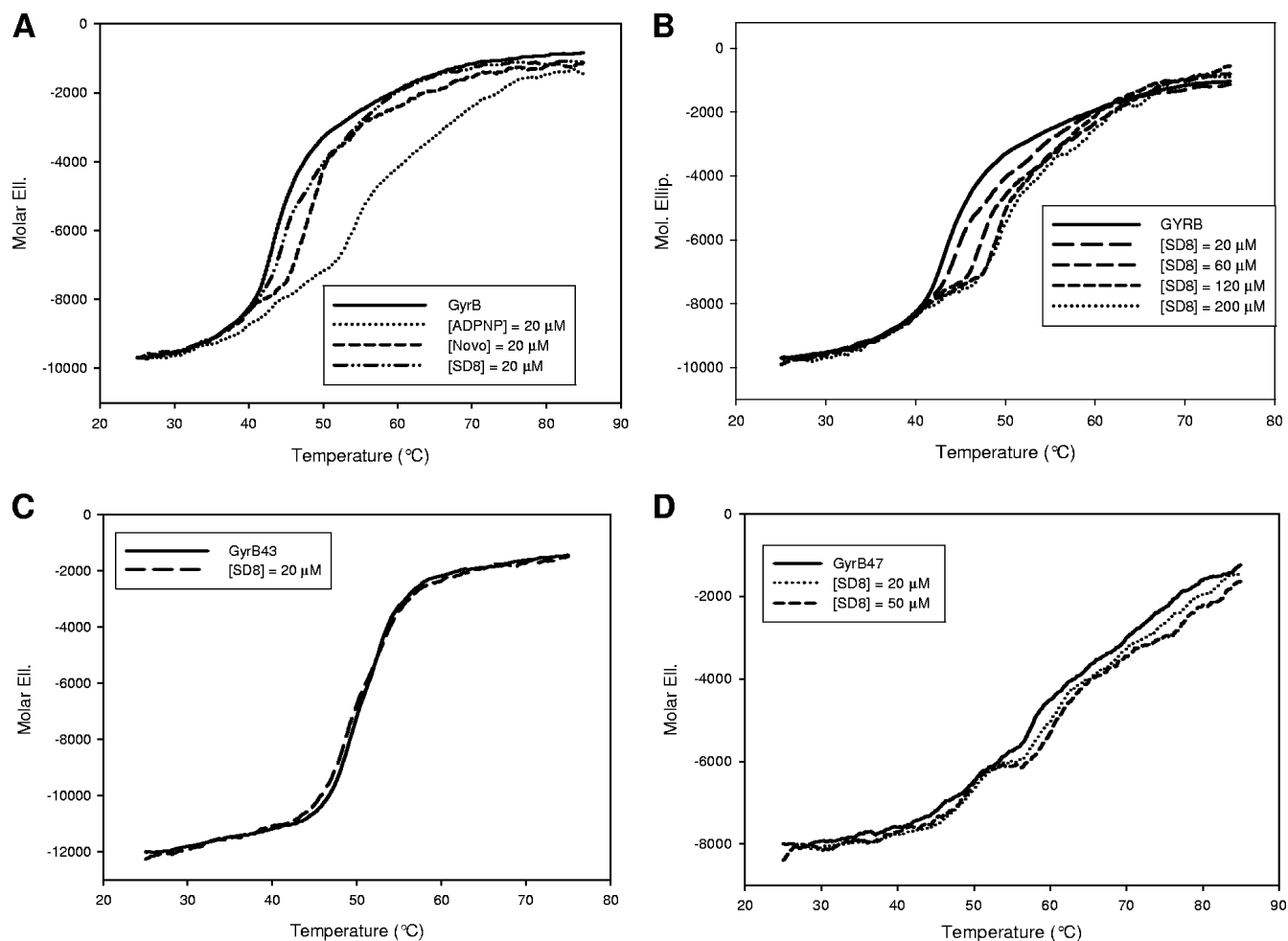


FIG. 4. Modulation of the melting profiles of GyrB and related subdomains acquired by recording the protein CD signal at 220 nm in 10 mM Tris-HCl (pH 7.5)–20 mM KCl–4 mM MgCl₂. (A) Effects of 20 μ M ligands on the melting profile of GyrB; (B) effects of increasing SD8 concentrations on the melting profile of GyrB; (C) effects of 20 μ M SD8 on the melting profile of GyrB43; (D) melting profile of GyrB47 in the presence or absence of SD8. The protein concentration was 0.2 μ M.

In particular, ADPNP, Novo, and SD8 produced a concentration-dependent increase in the T_m of GyrB, indicating a stabilization of the protein structure (Fig. 4A and B). The ligand-GyrB complexes exhibited distinct features in terms of the extent of thermal shift and the metal ion requirement (Fig. 5).

Interestingly, the temperature required to unfold the protein in the presence of ADPNP was strictly dependent upon Mg²⁺ (see Fig. S2 in the supplemental material). Indeed, under our experimental conditions, a maximal shift in the T_m was not observed in the absence of the divalent metal ion, thus supporting Mg²⁺-mediated ligand-protein interactions. In contrast, the interaction of SD8 and Novo with the protein was not sensitive to the presence or absence of Mg²⁺ in solution. This suggests a lack of any direct interaction between these drugs and divalent ions (data not shown). The difference in ΔT_m values recorded under the two conditions depends on the divalent metal ion effect on the protein melting profile (33). The ranking order for GyrB stabilization was Novo \geq ADPNP > SD8 (Fig. 5).

To identify the protein domain(s) actually involved in the drug binding process, similar experiments were performed with

the GyrB N- and C-terminal domains, GyrB43 and GyrB47, respectively. Interestingly, SD8 did not significantly affect the GyrB43 thermal transitions (Fig. 4C), whereas it effectively stabilized the native conformation of GyrB47 (Fig. 4D).

SD8 does not share its binding site(s) with coumarins. The data presented above show that there are distinct patterns of drug-mediated stabilization of each gyrase subunit. To further map possible overlaps of binding sites, we examined the protein melting profile obtained in the simultaneous presence of two of the ligands tested. Typical examples are reported in Fig. 6, in which the effects of the presence of two competitors (ADPNP and Novo; Fig. 6A) on GyrB are compared to those exhibited by two noncompetitive binders (ADPNP and SD8 [Fig. 6B] and Novo and SD8 [Fig. 6C]).

When Novo was added to the GyrB-ADPNP complex, a displacement of the nonhydrolyzable ATP analogue was observed. Indeed, the protein melting profile recorded in the presence of the two ligands was essentially identical to the one corresponding to the GyrB-ADPNP complex. Experiments performed with a constant ADPNP concentration in the presence of various amounts of Novo showed that nucleotide displace-

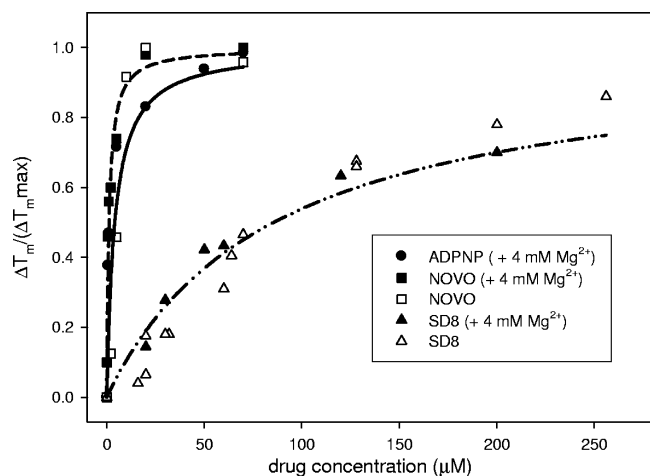


FIG. 5. Incremental variation of the melting temperature ($\Delta T/\Delta T_{\max}$, where ΔT is the change in temperature and ΔT_{\max} is the change in the maximum temperature) for the higher-temperature thermal transition of GyrB as a function of the ligand concentrations. The data refer to the melting profiles acquired by reading the CD signal at 220 nm in 10 mM Tris-HCl (pH 7.5)–20 mM KCl in the presence (full symbols) or the absence (empty symbols) of 4 mM MgCl_2 . In the presence of ADPNP, it was not possible to calculate this value when Mg^{2+} was not included in the buffer (see Fig. S1 in the supplemental material).

ment was directly related to the coumarin concentration and that it was complete at a 1:1 ADPNP/Novo ratio. In contrast, when ADPNP was added to the GyrB-SD8 complex, a GyrB thermal shift larger than the shifts obtained in the presence of the same concentrations of the single ligands was observed, which indicates an additive effect. The same was true for the Novo-SD8 system. In fact, by monitoring the effect of SD8 on the Novo-GyrB complex we were not able to observe coumarin displacement using up to a 10-fold excess of SD8, a range that includes equipotent drug concentrations. It should be noted that CFX was not able to displace any of the other ligands tested on GyrB. In fact, the melting profile of the ligand-enzyme mixture was not affected by the presence of the quinolone. The complete set of results is summarized in Table S1 in the supplemental material.

SD8 exhibits a unique GyrB proteolysis pattern. To further explore the GyrB-drug binding process, we analyzed the GyrB proteolysis pattern produced by trypsin and thermolysin in the presence or the absence of the drugs tested. Previous work showed that the tryptic digestion of GyrB initially produces the 43- and 47-kDa domains. GyrB43 is subsequently cleaved to a 33-kDa product that corresponds to the N-terminal domain, which is further extensively digested, whereas the 47-kDa product is rapidly digested to produce a main 25-kDa fragment that corresponds to the C-terminal sequence (2, 14).

A kinetic analysis of the GyrB digestion pattern in the pres-

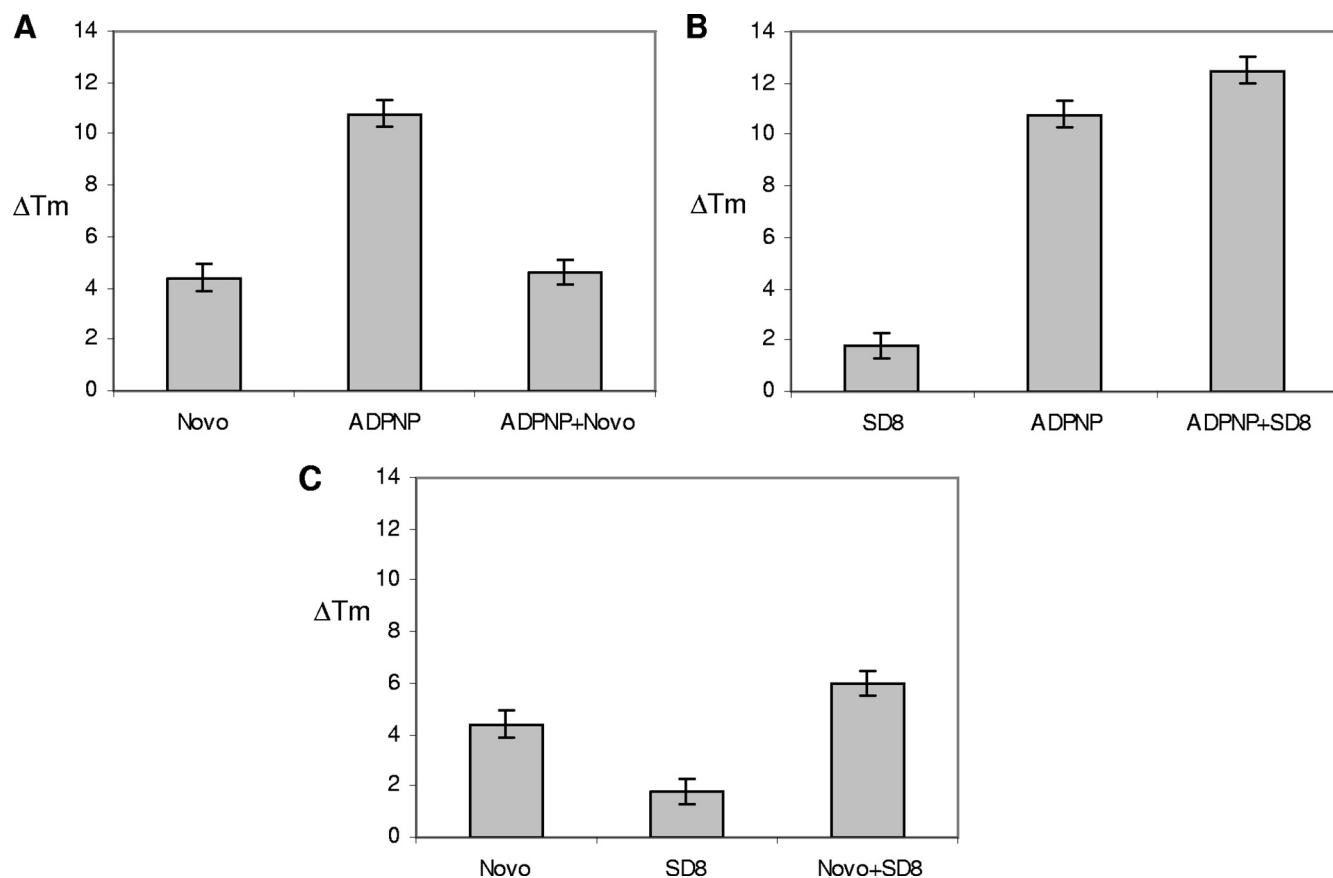


FIG. 6. Increments of GyrB melting temperature (ΔT) resulting from the protein CD signal at 220 nm in 10 mM Tris-HCl (pH 7.5)–20 mM KCl–4 mM MgCl_2 in the presence or the absence of different ligand (20 μM) combinations, as indicated.

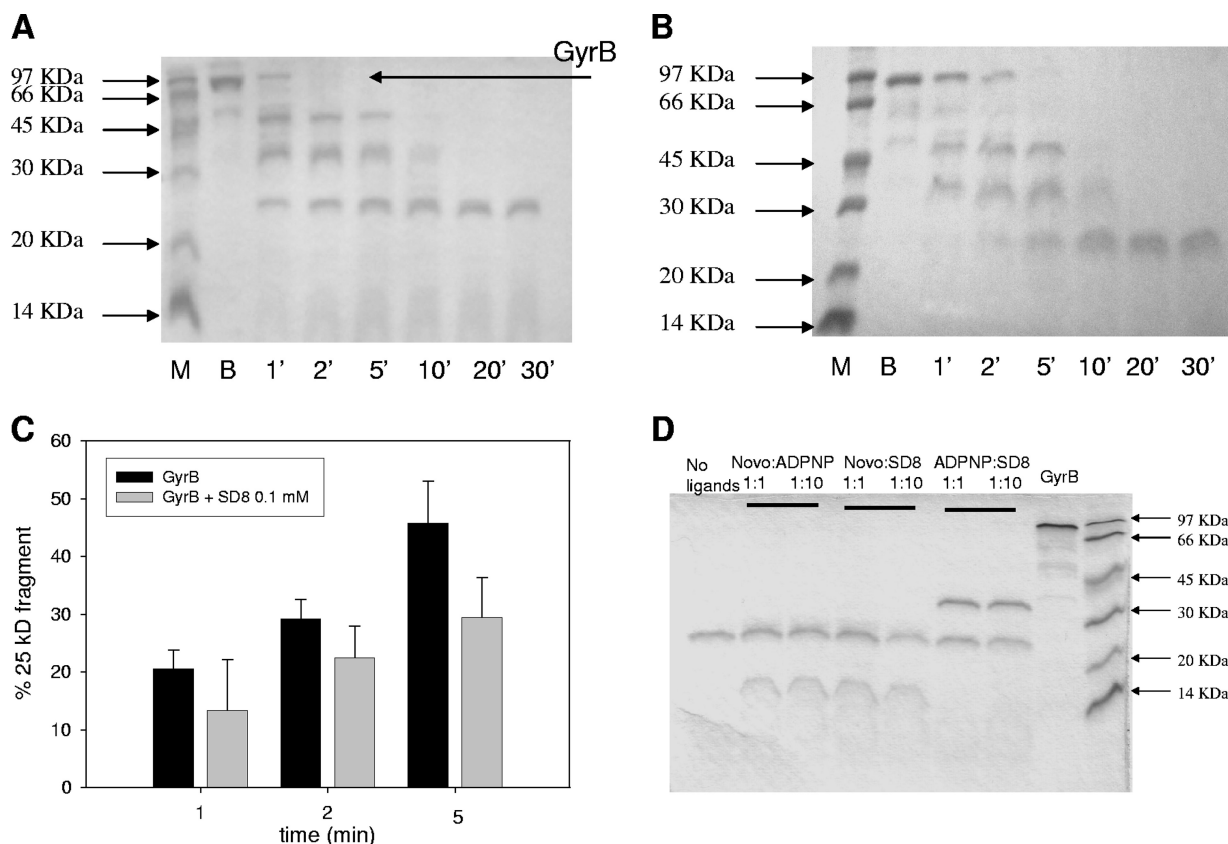


FIG. 7. Kinetics of GyrB (3 μ g) cleavage by trypsin in the absence (A) or the presence (B) of 100 μ M SD8. Lanes M, molecular mass markers; lanes B, GyrB in the absence of trypsin. (C) Quantitative determination of the 25 kDa GyrB fragment formation; (D) GyrB (3 μ g) cleavage patterns after 30 min of incubation with trypsin in the absence or the presence of the ligand (0.1 or 1 mM) combinations.

ence of the test drugs showed a modulation of the proteolytic pattern (Fig. 7A and B). In the presence of all test derivatives, the rate of disappearance of the full-length enzyme to produce subdomains GyrB43 and GyrB47 remained almost unchanged (see Fig. S3 in the supplemental material). This further supports the lack of extensive protein rearrangement, as shown by CD titrations. ADPNP stabilized the 33-kDa N-terminal domain, as evidenced by the presence of this fragment even after 30 min of incubation. Novo led to the formation of a 13-kDa fragment that, again, derives from digestion of the 43-kDa N-terminal domain (2, 14). Neither ADPNP nor Novo affected the digestion of the 47-kDa C-terminal domain; however, in the presence of SD8, the appearance of the 25-kDa proteolytic fragment was postponed. Although this effect was subtle, it supports a drug interaction with the C-terminal domain. A quantitative evaluation of the effects of SD8 on GyrB is reported in Fig. 7C.

When the protein was incubated with two-ligand combinations, SD8 did not affect the typical cleavage pattern produced by ADPNP or Novo up to a 10-fold molar excess, consistent with the presence of distinct binding sites on the B subunit (Fig. 7D). Comparable results (a distinct proteolytic pattern and no competition between SD8 and the other ligands) were observed by using thermolysin as the cleaving enzyme (data not shown).

Inhibition of gyrase by SD8 is not affected by the presence of Novo or ADPNP. All ligands tested are known to exhibit different mechanisms of interference with the catalytic activity of DNA gyrase. In particular, ADPNP and Novo compete for ATP binding and hydrolysis; hence, they efficiently reduce enzyme-mediated DNA supercoiling, whereas they do not significantly affect the enzymatic DNA relaxation activity (36). In contrast, SD8 efficiently inhibits gyrase-mediated DNA relaxation and supercoiling (7, 26). As a consequence, starting from a supercoiled plasmid, the efficiency of the relaxation process is related only to the activity of SD8, with the other ligands not contributing to the modulation of this reaction. These differences in the mechanisms of action allowed us to investigate the effects produced by drug combinations. In particular, we evaluated whether ADPNP and Novo could reduce the inhibitory activity of SD8. By applying these experimental protocols, we never observed a significant reduction in the inhibitory activity of SD8 as a function of the presence of Novo or ADPNP in solution (see Fig. S4 in the supplemental material).

SD8 prevents DNA from binding to DNA gyrase. Previous studies indicated that SD8 impairs gyrase binding to DNA (7). To confirm this, we determined the extent of Gyr-DNA complex formation by a gel shift assay (Fig. 8) using a pBR322 fragment (161 bp) containing the known gyrase hot spot at position 990 (18). When SD8 was added to the Gyr-DNA

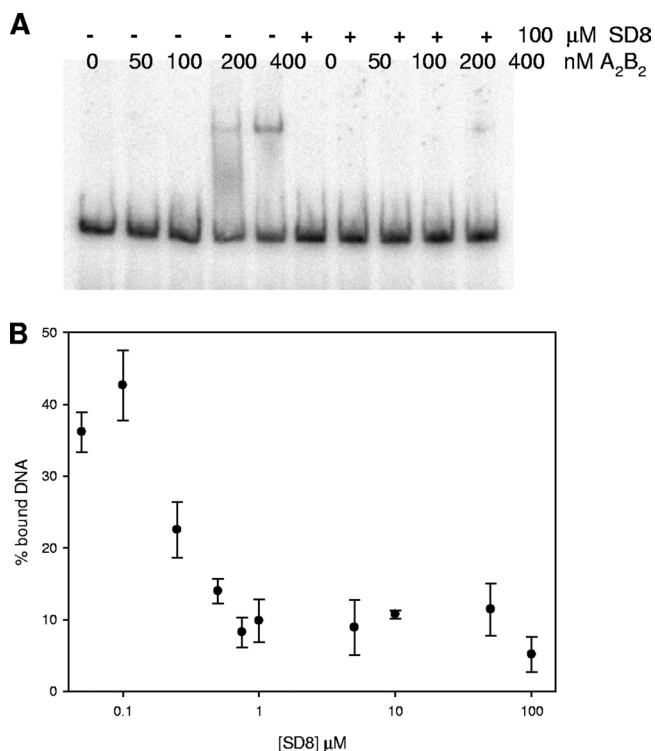


FIG. 8. Effect of SD8 on gyrase-DNA complex formation. DNA was incubated with increasing protein concentrations in the presence or the absence of 100 μ M SD8 (A). (B) The percentage of DNA bound by DNA gyrase (400 nM) as a function of the SD8 concentration in the reaction mixture. The buffer was made up of 10 mM Tris-HCl (pH 7.5), 20 mM KCl, and 4 mM MgCl₂.

reaction mixture, the formation of the DNA-protein complex was prevented in a drug concentration-dependent fashion. Interestingly, the amount of simocyclinone required to abolish DNA binding to the enzyme was in the low micromolar range, which is fully comparable to the amount necessary to suppress enzymatic activity *in vitro*. Spectroscopic evidence suggests that this effect is not due to a binary interaction of the drug with DNA (data not shown). This indicates that the SD8-Gyr complex is unable to appropriately recognize its DNA substrate.

DISCUSSION

Recently, simocyclinone D8 has attracted significant interest, as it represents a new antibiotic with an apparently novel mechanism of action that could be exploited for the rational design of potent chemotherapeutic agents (26, 29). In this connection, a detailed understanding of the molecular basis of the interaction of SD8 with its target is worthy of investigation. Recent work suggests that the antibiotic binds to the A subunit of the enzyme (6, 7). The results of our melting experiments with the N-terminal GyrA59 domain are fully consistent with this. An interesting feature of the binding process described above is represented by its S-shaped dependence upon the SD8 concentration (Fig. 3B). This indicates that under our experimental conditions, at least two SD8 molecules interact cooperatively per GyrA subunit. Interestingly, the conformational

transition window compares well with the SD8 concentrations needed to impair enzymatic activity, which suggests a correlation between drug-induced conformational change and enzyme inhibition.

Unexpectedly, additional binding of SD8 was seen on GyrB and, specifically, on the GyrB47 domain, which does not contain the ATP- and coumarin-binding sites. Considering that SD8, like Novo, contains an aminocoumarin ring, an overlapping binding site common to the two drugs might have been predicted. However, this is not the case, as confirmed by the lack of reciprocal displacement in competition experiments performed by the use of three different experimental approaches (protein thermal stability, proteolysis, and activity assays). This is consistent with the lack of interference of SD8 with the intrinsic ATPase activity of gyrase (7). It is worth recalling that in Novo the L-noviosyl sugar is implicated in competitive binding with the ATP adenine ring (17). Instead, SD8 contains a D-olivose deoxyhexose function, and additionally, its distance from the aminocoumarin moiety is changed in comparison to that of Novo. These major differences likely justify a change in the drug binding preference. In fact, the protein thermal stability and proteolysis assay data indicate that the SD8 binding site is totally unprecedented. A previous investigation failed to find evidence for an interaction of SD8 with GyrB (7). Indeed, surface plasmon resonance titrations were performed by using the GyrB43 domain only, which we confirmed did not contain any drug-binding sites. Isothermal titration calorimetry (ITC) titrations were performed with the full-length GyrB subunit. In this case, the lack of apparent binding might be related to a low reaction enthalpy. Additionally, at the high protein concentration required by the ITC technique (16 to 22 μ M), GyrB aggregation can occur (4), conceivably preventing drug recognition.

The two SD8 target domains on gyrase identified (GyrA59 and GyrB47) are known to be involved in DNA binding and protein-protein interactions. Although we do not know the exact location of the drug within GyrB47, the interaction could occur at the protein-protein interface, likely affecting the enzyme's local structure to render binding of DNA more difficult. Accordingly, experimental evidence confirmed that addition of the drug interferes with A₂B₂ recognition of DNA, thus impairing the proper generation of the cleavage complex and progression of the catalytic cycle.

However, the two sites are not equally effective in drug binding, the GyrA site exhibits a substantially higher affinity for SD8, as indicated by the melting experiments. At the moment, we do not have evidence indicating whether these two binding sites might be simultaneously operative. In any event, the assembly of GyrA and GyrB in the active form could possibly help to generate a more stable drug-protein complex. In this connection, protein thermal stabilization by SD8 is more notable on the reconstituted enzyme than on the isolated constituent subunits (Fig. 2 to 4), which suggests the potential cooperation of the two interaction events.

In conclusion, SD8 is not only characterized by a novel mechanism of action, but it may also represent the first DNA gyrase inhibitor directed toward two different target sites. The fact that simocyclinone is also active against cancer cell lines and inhibits human topoisomerase II (29) suggests that its mode of action is shared among several members of this family

of enzymes, which gives an opportunity to better understand the general features of drug-mediated enzyme poisoning and inhibition, as well as to rationally design new active drug prototypes.

ACKNOWLEDGMENTS

We gratefully acknowledge the financial support from the University of Padova (grant CPDA078422/07 to C.S.) and by AIRC, Milan, Italy (to M.P.). Work in A.M.'s laboratory was supported by the BBSRC (United Kingdom).

REFERENCES

1. Ali, J. A., A. P. Jackson, A. J. Howells, and A. Maxwell. 1993. The 43-kilodalton N-terminal fragment of the DNA gyrase B protein hydrolyzes ATP and binds coumarin drugs. *Biochemistry* **32**:2717–2724.
2. Ali, J. A., G. Orphanides, and A. Maxwell. 1995. Nucleotide binding to the 43-kilodalton N-terminal fragment of the DNA gyrase B protein. *Biochemistry* **34**:9801–9808.
3. Appelbaum, P. C., and P. A. Hunter. 2000. The fluoroquinolone antibacterials: past, present and future perspectives. *Int. J. Antimicrob. Agents* **16**:5–15.
4. Blandamer, M. J., B. Briggs, P. M. Cullis, A. P. Jackson, A. Maxwell, and R. J. Reece. 1994. Domain structure of *Escherichia coli* DNA gyrase as revealed by differential scanning calorimetry. *Biochemistry* **33**:7510–7516.
5. Drlica, K., M. Malik, R. J. Kerns, and X. Zhao. 2008. Quinolone-mediated bacterial death. *Antimicrob. Agents Chemother.* **52**:385–392.
6. Edwards, M. J., R. H. Flatman, L. A. Mitchenall, C. E. Stevenson, T. B. K. Le, H. P. Fiedler, A. R. McKay, T. A. Clarke, M. J. Buttner, D. M. Lawson, and A. Maxwell. A crystal structure of the bifunctional antibiotic, simocyclinone D8, bound to DNA gyrase. *Science*, in press.
7. Flatman, R. H., A. J. Howells, L. Heide, H. P. Fiedler, and A. Maxwell. 2005. Simocyclinone D8, an inhibitor of DNA gyrase with a novel mode of action. *Antimicrob. Agents Chemother.* **49**:1093–1100.
8. Galm, U., J. Schimana, H. P. Fiedler, J. Schmidt, S. M. Li, and L. Heide. 2002. Cloning and analysis of the simocyclinone biosynthetic gene cluster of *Streptomyces antibioticus* Tu 6040. *Arch. Microbiol.* **178**:102–114.
9. Gellert, M., K. Mizuuchi, M. H. O'Dea, and H. A. Nash. 1976. DNA gyrase: an enzyme that introduces superhelical turns into DNA. *Proc. Natl. Acad. Sci. U. S. A.* **73**:3872–3876.
10. Gellert, M., K. Mizuuchi, M. H. O'Dea, H. Ohmori, and J. Tomizawa. 1979. DNA gyrase and DNA supercoiling. *Cold Spring Harbor Symp. Quant. Biol.* **43**(Pt 1):35–40.
11. Gormley, N. A., G. Orphanides, A. Meyer, P. M. Cullis, and A. Maxwell. 1996. The interaction of coumarin antibiotics with fragments of DNA gyrase B protein. *Biochemistry* **35**:5083–5092.
12. Heddle, J. G., F. M. Barnard, L. M. Wentzell, and A. Maxwell. 2000. The interaction of drugs with DNA gyrase: a model for the molecular basis of quinolone action. *Nucleosides Nucleotides Nucleic Acids* **19**:1249–1264.
13. Holzenkammer, M., M. Walker, A. Zeeck, J. Schimana, and H. P. Fiedler. 2002. Simocyclinones, novel cytostatic angucyclinone antibiotics produced by *Streptomyces antibioticus* Tu 6040 II. Structure elucidation and biosynthesis. *J. Antibiot. (Tokyo)* **55**:301–307.
14. Kampranis, S. C., and A. Maxwell. 1998. Conformational changes in DNA gyrase revealed by limited proteolysis. *J. Biol. Chem.* **273**:22606–22614.
15. Laponogov, I., M. K. Sohi, D. A. Veselkov, X. S. Pan, R. Sawhney, A. W. Thompson, K. E. McAuley, L. M. Fisher, and M. R. Sanderson. 2009. Structural insight into the quinolone-DNA cleavage complex of type IIA topoisomerases. *Nat. Struct. Mol. Biol.* **16**:667–669.
16. Lee, C. 2008. Therapeutic challenges in the era of antibiotic resistance. *Int. J. Antimicrob. Agents* **32**(Suppl. 4):S197–S199.
17. Lewis, R. J., O. M. Singh, C. V. Smith, T. Skarzynski, A. Maxwell, A. J. Wonacott, and D. B. Wigley. 1996. The nature of inhibition of DNA gyrase by the coumarins and the cyclothialidines revealed by X-ray crystallography. *EMBO J.* **15**:1412–1420.
18. Lockshon, D., and D. R. Morris. 1985. Sites of reaction of *Escherichia coli* DNA gyrase on pBR322 in vivo as revealed by oxolinic acid-induced plasmid linearization. *J. Mol. Biol.* **181**:63–74.
19. Maxwell, A. 1999. DNA gyrase as a drug target. *Biochem. Soc. Trans.* **27**:48–53.
20. Maxwell, A. 1993. The interaction between coumarin drugs and DNA gyrase. *Mol. Microbiol.* **9**:681–686.
21. Maxwell, A., and D. M. Lawson. 2003. The ATP-binding site of type II topoisomerases as a target for antibacterial drugs. *Curr. Top. Med. Chem.* **3**:283–303.
22. Mulvey, M. R., and A. E. Simor. 2009. Antimicrobial resistance in hospitals: how concerned should we be? *CMAJ* **180**:408–415.
23. Noble, C. G., and A. Maxwell. 2002. The role of GyrB in the DNA cleavage-religation reaction of DNA gyrase: a proposed two metal-ion mechanism. *J. Mol. Biol.* **318**:361–371.
24. Nollmann, M., N. J. Crisona, and P. B. Arimondo. 2007. Thirty years of *Escherichia coli* DNA gyrase: from in vivo function to single-molecule mechanism. *Biochimie* **89**:490–499.
25. Oblak, M., M. Kotnik, and T. Solmajer. 2007. Discovery and development of ATPase inhibitors of DNA gyrase as antibacterial agents. *Curr. Med. Chem.* **14**:2033–2047.
26. Opegard, L. M., B. L. Hamann, K. R. Streck, K. C. Ellis, H. P. Fiedler, A. B. Khodursky, and H. Hiasa. 2009. In vivo and in vitro patterns of the activity of simocyclinone D8, an angucyclinone antibiotic from *Streptomyces antibioticus*. *Antimicrob. Agents Chemother.* **53**:2110–2119.
27. Palumbo, M., B. Gatto, G. Zagotto, and G. Palu. 1993. On the mechanism of action of quinolone drugs. *Trends Microbiol.* **1**:232–235.
28. Reece, R. J., and A. Maxwell. 1991. DNA gyrase: structure and function. *Crit. Rev. Biochem. Mol. Biol.* **26**:335–375.
29. Sadiq, A. A., M. R. Patel, B. A. Jacobson, M. Escobedo, K. Ellis, L. M. Opegard, H. Hiasa, and R. A. Kratzke. 10 January 2009, posting date. Anti-proliferative effects of simocyclinone D8 (SD8), a novel catalytic inhibitor of topoisomerase II. *Invest. New Drugs* [Epub ahead of print.].
30. Schimana, J., H. P. Fiedler, I. Groth, R. Sussmuth, W. Beil, M. Walker, and A. Zeeck. 2000. Simocyclinones, novel cytostatic angucyclinone antibiotics produced by *Streptomyces antibioticus* Tu 6040. I. Taxonomy, fermentation, isolation and biological activities. *J. Antibiot. (Tokyo)* **53**:779–787.
31. Schoeffler, A. J., and J. M. Berger. 2008. DNA topoisomerases: harnessing and constraining energy to govern chromosome topology. *Q. Rev. Biophys.* **41**:41–101.
32. Sissi, C., A. Chemello, E. Vazquez, L. A. Mitchenall, A. Maxwell, and M. Palumbo. 2008. DNA gyrase requires DNA for effective two-site coordination of divalent metal ions: further insight into the mechanism of enzyme action. *Biochemistry* **47**:8538–8545.
33. Sissi, C., E. Marangon, A. Chemello, C. G. Noble, A. Maxwell, and M. Palumbo. 2005. The effects of metal ions on the structure and stability of the DNA gyrase B protein. *J. Mol. Biol.* **353**:1152–1160.
34. Sissi, C., E. Perdona, E. Domenici, A. Feriani, A. J. Howells, A. Maxwell, and M. Palumbo. 2001. Ciprofloxacin affects conformational equilibria of DNA gyrase A in the presence of magnesium ions. *J. Mol. Biol.* **311**:195–203.
35. Song, J. H. 2008. What's new on the antimicrobial horizon? *Int. J. Antimicrob. Agents* **32**(Suppl. 4):S207–S213.
36. Sugino, A., N. P. Higgins, P. O. Brown, C. L. Peebles, and N. R. Cozzarelli. 1978. Energy coupling in DNA gyrase and the mechanism of action of novobiocin. *Proc. Natl. Acad. Sci. U. S. A.* **75**:4838–4842.
37. Sugino, A., C. L. Peebles, K. N. Kreuzer, and N. R. Cozzarelli. 1977. Mechanism of action of nalidixic acid: purification of *Escherichia coli* nalA gene product and its relationship to DNA gyrase and a novel nicking-closing enzyme. *Proc. Natl. Acad. Sci. U. S. A.* **74**:4767–4771.
38. Theobald, U., J. Schimana, and H. P. Fiedler. 2000. Microbial growth and production kinetics of *Streptomyces antibioticus* Tu 6040. *Antonie Van Leeuwenhoek* **78**:307–313.